Available online at www.sciencedirect.com
ScienceDirect
Physica C 454 (2007) 82–87
PHYSICA C
www.elsevier.com/locate/physc

Raman analysis of asymmetrical chains in $YBa_2Cu_3O_{7-\delta}$ films

Seongsik Hong *, Kyungmoon Kim, Hyeonsik Cheong, Gwangseo Park

Department of Physics, Sogang University, Seoul 121-742, Republic of Korea

Received 13 February 2006; received in revised form 19 January 2007; accepted 4 February 2007
Available online 12 February 2007

Abstract

$YBa_2Cu_3O_{7-\delta}$/MgO(1 0 0) thin films with depletion of oxygen have been studied with Raman spectroscopy. The depletion changes the intensity of 233 and 596 cm^{-1} phonons induced from Cu(1)–O(1) asymmetrical chains. A simple model of a symmetry-broken chain row is introduced to explain this phenomenon. With depletion, the row is configured as asymmetrical [O(1)–Cu(1)–o(1)] chains, where O(1) and o(1) are full and deficient oxygen in the orthorhombic and tetragonal structures, respectively. The Raman peaks at 233 and 596 cm^{-1} increase with an increase in a population density of the asymmetrical chains in the row and decrease as the row has more symmetric sites of full or deficient oxygen. As a result, the intensity of the chain-induced modes reflects a degree of the opposite structure involved in the phase transition in a single-phase film, which is verified by both the relative intensity of the 232 cm^{-1} phonon and the full width at half maximum of a Cu(2) superposition band from the coexisting phases in the film. All the results support the asymmetrical-chain model.

PACS: 74.72.−h; 74.72.Bk; 74.78.Bz

Keywords: YBCO; Asymmetrical chains; Raman spectroscopy

1. Introduction

The photoinduced superconductivity of $YBa_2Cu_3O_x$ (YBCO) is explained by the photocreation of electron–hole pairs with the trapping of carriers in O vacancies [1,2] or by oxygen ordering in the Cu(1)–O(1) chains [3–6]. It is well known that the illumination of visible light on YBCO has a strong effect on the resonance of the chain-related modes which are optically bleached for the spectral photon energies [7]. In general, the Raman-forbidden modes that are identical to phonons observed in O-deficient chains are characterized by the polarizability of incident light in the Cu(1)–O(1) chain direction [8]. Due to the high O(1) mobility, laser annealing of YBCO films reduces the chain-oxygen content inside a spot area and results in broken symmetry of the chain sites, which strongly modifies the polarizable modes assigned to Cu(1) and O(1) vibrations [9,10]. As markers for the existence of the vibrations and the development of a photoexcitation/oxygen-reordering model, most studies have suggested fragment chains which originate from oxygen-vacant sites in the long Cu(1)–O(1) arrangements [9–12]. However, the fragment model is problematic because the description of the origin for the Cu(1) and O(1) phonons is ambiguous. Most of available experimental data are not informative enough to convincingly confirm their vibration modes. Particularly, the oxygen-vacant chain Cu(1)–Cu(1) in the *b*-direction raises a serious question on the crystal structure since the atomic vacancy may not be recovered by a proper treatment, and it might be a permanent defect in the chains. The recovery in an adequate condition is one of the most characteristic properties observed in YBCO materials [13–16], and oxygen reordering is linked to the orthorhombic/tetragonal structural phase transition [17]. Therefore, more study on the modes from Cu(1)–O(1) chains in YBCO crystals is needed with Raman spectroscopy.

In this study we focuses on a structural feature of CuO asymmetrical chains in deoxygenated films with

* Corresponding author. Tel./fax: +82 02 703 7737.
E-mail address: sungsikh@hanafos.com (S. Hong).

0921-4534/$ - see front matter © 2007 Elsevier B.V. All rights reserved.
doi:10.1016/j.physc.2007.02.001

post-growth annealing in the vacuum chamber. Unlike studies in selected oxygen concentration samples, our measurements are carried out on films with continuous depletion. A progressive change of the oxygen content contributes to the orthorhombic/tetragonal phase transition, and a model of Cu(1)–O(1) rows is introduced to explain intensity variations of induced modes from the symmetry-broken chains which are linked to oxygen reordering during the phase transition.

2. Experimental

YBCO materials were deposited on clean MgO(100) substrates at 760 °C in a 500-mTorr O_2 pressure, using a 248-nm KrF-excimer laser adjusted to 210 mJ per pulse with a frequency of 3 Hz. The as-grown films were annealed at 500 °C for 2 h in a 500-Torr O_2 pressure. The film thickness measured by transmission electron microscopy was about 200 nm. Transition temperatures and current densities at 77 K for the fully oxygenated films were 87–89 K and around 10^6 A cm^{-2}, respectively. From θ–2θ scans by X-ray diffraction, only c-orientations were detectable. After the characterizations, oxygen in the films was depleted at 300–325 °C for 2–25 min in a vacuum environment of $\sim 10^{-5}$ Torr. An increasing rate to the depletion temperature was 20 °C per min, followed by natural cooling. These depletion processes were repeated after Raman spectra were taken from the films at room temperature in the quasi-backscattering geometry, using the 514.5-nm line of a 50-mW argon-ion laser focused to a line of 5 mm × 0.1 mm as the excitation source. The irradiation on the large area during the Raman measurements did not result in a change for the oxygen content. The signal was dispersed by a Spex 0.55-m spectrometer with a holographic edge filter and detected by a charge-coupled-device (CCD) detector array cooled with liquid nitrogen. The intensity of the Raman signal depends on the sample orientation and the polarizable direction of incident and scattered light. In these measurements we do not distinguish between the x and y polarizations of the reflected signal. Therefore, the Raman intensity of a band in a film is nearly as strong as the $(xx) + (yy)$ average measured in the samples [7].

3. Results and discussion

Fig. 1 shows a series of typical Raman spectra for the various oxygen content (x) related to a frequency of the apical O(4) mode [18–20]. Spectrum (a) has been taken from a sample of the fully oxygenated films. The modes observed in this spectrum are almost normal Raman-active phonons in the CuO_2 planes: Cu(2)-A_g at 151 cm^{-1}, out-of-phase O(2,3)-B_{1g} at 339 cm^{-1}, and in-phase O(2,3)-A_g at 435 cm^{-1}. The apical O(4) mode is seen at 501 cm^{-1}. All the frequencies are well known phonons recorded in the orthorhombic structure [20–22]. Our edge filter has a detection limit around 136 cm^{-1}, and thus the Ba-A_g mode at 115 cm^{-1} is not shown.

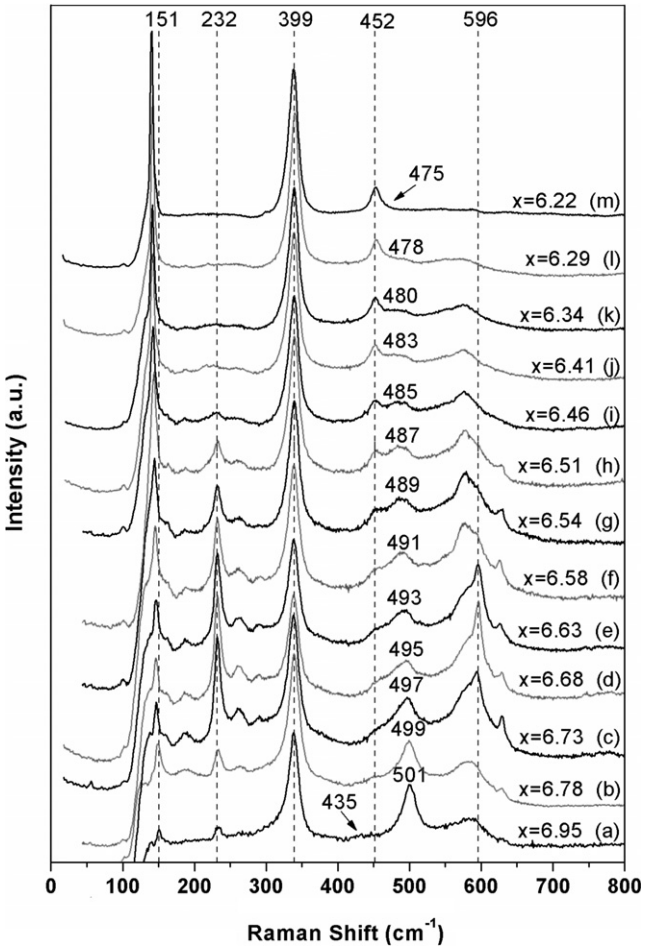

Fig. 1. Spectral variations for oxygen content (x). Spectrum (a) has been taken from a fully oxygenated film and spectra (b)–(i) taken from the oxygen-deficient film obtained by thermal annealing in vacuum.

As oxygen is depleted, dramatic changes associated with the oxygen content are observed in the spectra. The main change induced by the oxygen depletion is a strong enhancement of lines at 232 and 596 cm^{-1} which are attributed to the vibrations of Cu(1) and O(1) atoms [9]. The center vibration at 587 cm^{-1} of the O(1) band in spectrum (a) blueshifts to 596 cm^{-1} in spectrum (d) with a shoulder at 586 cm^{-1}, which is one of the most interesting observations at the stages between (a) and (d) because the center phonon of the O(1) band redshifts in the other spectra. Further depletion of the film makes the apical mode shift to 491 cm^{-1} in spectrum (f), reducing the weight of the sharp peak on the O(1) band. The intensity of O(2,3)-B_{1g} mode along with Cu(2)-A_g mode increases, and the Cu(1) mode weakens. On further lowering of the oxygen content, a remarkable reduction of the Cu(1) mode is observed in spectrum (i) with a loss of the sharp peak on the O(1) band. For the depletion between spectra (g) and (l), the O(4) mode shifts to 489–478 cm^{-1}. The final depletion leads to the complete disappearance of the induced phonons as seen in spectrum (m) and to the enhancement of vibrations in the CuO_2 planes: O(2,3)-B_{1g} at 340 cm^{-1}, O(2,3)-A_g at

452 cm^{-1}, and Cu(2)-A_g at 141 cm^{-1}. All the frequencies are conventional phonons found in the YBCO tetragonal phase [22,23].

The intensity of the mode at 232 cm^{-1} seems to vary with a spectral weight of the sharp peak on the broad band centered at 596 cm^{-1}. Their variation in correlation with each other provide solid information on asymmetrical chains that are related to the ordering of deficient chain-sites of tetragonal unit cells appearing due to depletion of fully oxygenated ones in orthorhombic unit cells. Additionally, the progressive disappearance of the apical mode is attributed to a migration of oxygen towards the empty O(5) positions in the *a*-axis. This disordering of the oxygen atoms destroys the one-dimensional chains and results in a two-dimensional layer. In the tetragonal structure the corresponding sites at $(1/2,0,0)$ and $(0,1/2,0)$ are symmetric and thus are equally occupied [17]. Fig. 2(a) shows the lattice structures of the chain basal planes for the orthorhombic unit cells in *Pmmm* space group and the tetragonal unit cells in *P4/mmm* space group. To understand the origin of the 232 cm^{-1} and 596 cm^{-1} modes, it is highly desirable to appreciate asymmetrical ordering of Cu(1)–O(1) chains along the *b*-axis. To do this and to explain intensity variations of the Raman-induced phonons when the chain sites of oxygen deficiency increase, we introduce here a model of a chain row in ten YBCO-unit cells. Fig. 2(b) depicts the scenarios. There are two chain atoms, Cu and O, per unit cell. A large solid circle stands for a Cu(1) atom. A medium open circle represents an O(1) atom in the orthorhombic phase of the fully oxygenated sites, and a small solid circle expresses an o(1) atom in the tetragonal phase of the oxygen-deficient ones. Therefore, O(1) and o(1) stands for full and deficient oxygen, respectively. It is possible to make a lot of asymmetrical ordering combination in a row, but the configurations are regularized for a plausible approach to interpretation of the spectra.

Suppose that the oxygen-deficient site increases by one at every step from row (0) of fully oxygenated sites. Then, the asymmetrical ordering is maximized when a chain row is balanced with alternately full and deficient sites as in row (5) in which orthorhombic (metallic) and tetragonal (insulating) unit cells are equal in number. This row can be configured as 5 linear [O(1)–Cu(1)–o(1)]s with 5 [Cu(1)]s between the two linear structures. It can be also described as a different systematic way to constitute 5 [Cu(1)–O(1)–Cu(1)]s with 5 [o(1)]s or 5 [Cu(1)–o(1)–Cu(1)]s with 5 [O(1)]s. The first configuration is more plausible because of the detection of vibration modes from a loss of the left–right symmetry. The asymmetrical linear structure, [O(1)–Cu(1)–o(1)], will be termed *orthotetra* chain hereafter since O(1) and o(1) are chain oxygen in orthorhombic and tetragonal unit cells, respectively. As deficiency increases from row (5), the population of the *orthotetra* chain decreases conversely with more ordered insulating chains. The final process makes all the chains being in complete deficiency as in row (10).

Fig. 3 represents chains configured in the chain rows of the YBCO unit cells. The O(1)–Cu(1)–O(1) and o(1)–Cu(1)–o(1) structures in Fig. 3(a) and (b) are symmetric. The bond dipoles in opposite directions have equal size. The stretches of the symmetrical chains along the *b*-axis do not induce a transient dipole moment. No active chain mode is expected in these motions due to the selection rules. On the other hand, Fig. 3(c) and (d) show asymmetrical vibrations around atomic equilibrium positions in the polar *orthotetra* chain of which the bond dipoles do not cancel each other out. In chains with little or no symmetry, modes are likely to be active in both IR and Raman spectroscopy. The transition dipole moment and induced polarizability in the *b*-direction for the *orthotetra* chain oscillate with a frequency of the impinging radiation. There exist two distinct frequencies directly corresponding to the asymmetrical vibrations because a unique motion has a characteristic normal mode. Other published reports on the chain modes, often called induced modes, have assigned 232 cm^{-1} and 596 cm^{-1} phonons to Cu(1) and O(1) modes [9,10]. Armed with the semiempirical or theoretical idea [24–26], a simple calculation of the Raman tensor can be conducted on the normal coordinates of the *b*-direction. The Raman polarizability must have one component α_{yy} related to the modes at 232 and 596 cm^{-1}. The length of the arrows is proportional to the displacement of the atoms. For the 232 cm^{-1} mode we can expect a somewhat stronger dependence on the atomic mass since the Cu atom involves small displacements of the O–Cu or Cu–o in this mode. The oxygen is not expected to have a strong influence on that vibration. The 596 cm^{-1} mode are mainly described as asymmetrical-oxygen stretches. The changes

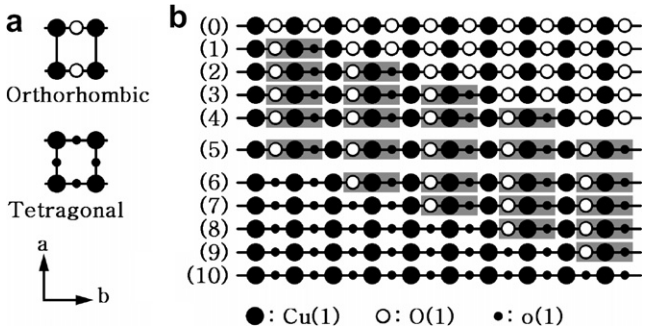

Fig. 2. (a) Lattice structures of the chain basal planes in the orthorhombic and tetragonal unit cells. (b) Scenarios of the phase transition of a chain row in ten-unit cells as the chain sites of oxygen deficiency increase, where the gray parts represent asymmetrical O(1)–Cu(1)–o(1) chains.

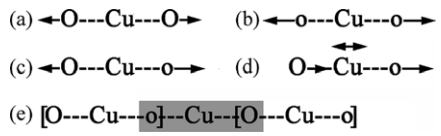

Fig. 3. Chain configurations and motions in the *b*-direction. (a) A chain of fully oxygenated sites in orthorhombic unit cells. (b) A chain of deficient sites in tetragonal unit cells. (c) and (d) Stretch motions of the *orthotetra* chain. (e) Bonding of a Cu(1) atom between two *orthotetra* chains.

in asymmetrically ionic radius dominate over the displacements of the Cu atom. In such considerations, the 596 cm^{-1} and 232 cm^{-1} phonons are matched to the vibrations of Fig. 3(c) and (d), respectively. The Cu(1) atom between two *orthotetra* chains configures oxygen bonding like the gray part in Fig. 3(e). This bonding structure, [o–Cu–O], is reversibly same as the *orthotetra* chain. Its vibrations are also included in the asymmetrical motions of Fig. 3(c) and (d).

Row (0) in Fig. 2 has no *orthotetra* chain. All the chains are symmetric with fully oxygenated sites. A film with such a row is in a highly ordered state of the orthorhombic phase. Spectrum (a) in Fig. 1, detected from the fully oxygenated film, may reflect this situation and show only phonons vibrating from the orthorhombic unit cells with symmetrical O(1)–Cu(1)–O(1) chains as in row (0) which is IR/Raman-inactive. However, small intensities of the induced modes are observed in this spectrum. It is appreciated that intrinsic deficient or defect chains exist initially. Impurities, substrate defects, mismatch, local disorder, etc., all of them are hampers to an epitaxial growth. The chain-induced modes will be stronger if population of the *orthotetra* chain increases in a row. Spectra (b) and (c) in Fig. 1, measured for the first and second depletion, imply these conditions. For ideal depletion, the *orthotetra* chain is most dominated as in row (5). Many *orthotetra* fragments have vibrations that occur within a relatively narrow range of the frequencies. This concept is experimentally supported by the phonons observed in spectrum (d) in Fig. 1. The sharp peaks of the 232 and 596 cm^{-1} phonons can be explained based on a high population density of the asymmetrical O(1)–Cu(1)–o(1) chains. A blueshift to 596 cm^{-1} is associated with many *orthotetra* chains in the film. There is a particular tendency that the depletion for spectrum (d) in Fig. 1 raises the background scattering of a frequency range between 210 and 400 cm^{-1}. Such a dynamic change may occur if the maximized asymmetrical distribution like row (5) in Fig. 2 is considered between the chains and the *ab*-planes. A first physical feature of such a film is a serious suppression of superconductivity since the tetragonal sites are involved in the nonsuperconducting state. As deficiency increases from row (5), on the other hand, the number of the *orthotetra* chain decreases with the symmetrical-chain sites of tetragonal unit cells. Therefore, more ordered insulating chains in the film result in a reduction of the chain-induced modes, which is confirmed by the decrease in spectra (e)–(h) in Fig. 1. With complete deficiency, no induced mode would be expected because the row has only symmetrical o(1)–Cu(1)–o(1) chains which are also IR/Raman-inactive. This oxygen-depleted film is in another highly ordered state of the tetragonal phase as in row (10) that is opposite to the orthorhombic one as in row (0). This is verified by the fact that the final depletion for spectrum (m) in Fig. 1 leads to the disappearance of the chain modes. The spectrum shows only phonons vibrating from the tetragonal unit cells. As a result, the induced modes of the *orthotetra* chains show that their intensities reflect a degree of the opposite structure during a phase transition in a single-phase film.

To evaluate the phase transition by the intensities, we have normalized the spectral weight of the symmetrical Cu(1) mode (232 cm^{-1} phonon) with respect to the intensity of O(2,3)-B_{1g}. In this calculation the O(1) mode (596 cm^{-1} phonon) was not used because this mode is very broad and its base line fluctuates. Fig. 4 shows the variations of the normalized Cu(1) intensity ratio, $R = I_{Cu(1)}/I_{B_{1g}}$, which follows a Lorenzian distribution as a function of the oxygen content. The largest value appears in the vicinity of $x = 6.68$. The values of single-phase regions at the ends of the x-axis are suppressed to be almost negligible, as expected. These results of the Cu(1) mode for the asymmetrical Cu–O rows provide a clear indication regarding the phase transition in YBCO superconductors, and the single-phase assessment based on the spectral weight of Cu(1) is by no means ambiguous. The inset of Fig. 4 shows frequency shifts of the O(1) mode as a function of the oxygen content. Before and after chain row (5) in Fig. 2, the O(1) frequency can be modulated by the formation of the various deficient ordering in the Cu–O chains. Upon depletion, full oxygen sites are randomly converted into deficient sites, and thus the distribution of *orthotetra* chains over a film is inhomogeneous. The shift of the O(1) mode is believed to be associated with a degree of the homogeneity of *orthotetra* chains. On the other hand, the Cu(1) mode from interacting with asymmetrical neighbors is supposed to be less affected by their surroundings since the Cu(1)-induced mode is almost invariant at its own position.

Direct information on the phase transition is found in the splitting of Cu(2) phonons into two frequencies of 141 and 151 cm^{-1} as seen in the inset of Fig. 5, which are often observed in the spectra between (c) and (g) in Fig. 1. They are well known phonons from vibrations of Cu(2) atoms in the respective insulating and metallic structures [27,28]. However, it is hard to see the double peaks in most data because the two peak frequencies are within

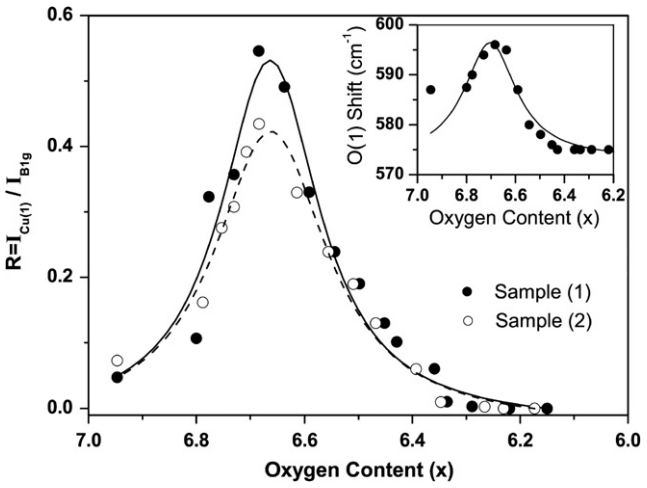

Fig. 4. Variations of the relative intensity of the Cu(1) mode versus oxygen content. The inset shows frequency shifts of the O(1) mode.

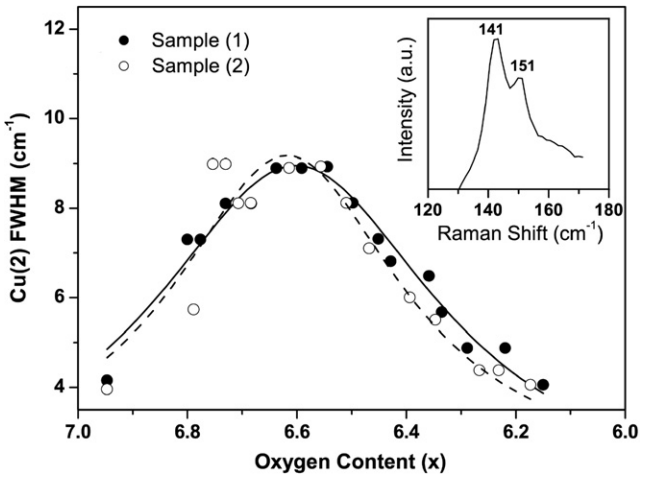

Fig. 5. A plot of the full width at half maximum (FWHM) of the Cu(2) band. The inset shows a splitting of the phonons into two frequencies of 141 and 151 cm^{-1}. The former is the phonon of Cu(2) atoms in the insulating structure, and the latter in the metallic structure.

10 cm^{-1}, and the individual phonons can scarcely be resolved. A spectral bandwidth with the superposition of coexisting phases of which relative weight is determined by their abundance in a film can be broader when compared with their single band. Fig. 5 is a plot of the full width at half maximum (FWHM) of the superposition band from the vibrations of Cu(2) atoms in the CuO_2 planes. The FWHM at $x = 6.62$ is almost two times greater than the values of the left–right end points representing the single phases. This result is believed to originate from a situation of the phonons vibrating from the two single structures balanced by each other in the film. The decreasing width with decreasing oxygen content implies that the insulating cells are increasing in the decreasing metallic-cells. The two independent vibrations in the transition region exist clearly, and the inclination of the trace is exactly in accordance with the theoretical predictions in Fig. 2.

The origin of the induced modes from the Cu(1)–O(1) chains has been a matter of continued debate. In many reports the activated Raman modes are explained in terms of resonant processes at electronic states localized at vacant-chain ends [6,11,12]. In the latest study [3] on bidirectional photoswitching associated with the CuO chains in oxygen-deficient YBCO single crystals, a charge transfer transition in the chain fragments takes part in a resonance Raman process, and an intensity maximum of the fragment-chain-end phonons from randomly distributed oxygen vacancies is at around $x = 6.7$ which agrees well with the value in Fig. 5 except for the origin. An early report on intermediate oxygen concentrations [29] suggested the Ortho II phase of the $Y_2Ba_4Cu_60_{13}$ structure which corresponds to a doubling of the unit cell based on the vacant-chain sites. Its Raman spectrum from the Ortho II phase is consistent with Fig. 1(d) appearing when the *orthotetra* chains are most populated during the phase transition as in row (5) of Fig. 2. Returning to the data in Fig. 4 matched with the analysis in Fig. 2, we see that the intensity of the induced modes in an intermediate state during the phase transition increases with increasing population densities of the asymmetrical *orthotetra* chains with no oxygen vacancy. In the early neutron-powder-diffraction measurement [17], the phase transition is continuous disordering of oxygen atoms, which brings the destruction of novel one-dimensional Cu–O chains for the orthorhombic structure to the formation of two-dimensional Cu–O planes for the tetragonal structure.

4. Conclusion

Our asymmetrical-chain model can be summarized as follows. First, the stretches of the O(1)–Cu(1)–o(1) *orthotetra* chain have two individual modes depending on the transient dipole moment or polarizability from the structural asymmetry. Second, deficient chains in the model can be easily converted into full-oxygen chains at a proper annealing temperature and O_2 pressure, i.e., under an adequate condition, oxygen-deficient chains of tetragonal cells are transformed into full-oxygen ones of orthorhombic cells and *vice versa*. Therefore, intensities of the induced modes reflect a degree of an opposite structure in a single-phase film. Third, the phase transition randomly takes place over a film, and thus a degree of asymmetrical-chain order may be different, which causes the broadening and shifts of the O(1) band.

Acknowledgement

This work was supported by the Korea Research Foundation Grant funded by the Korean Government (MOEHRD) (KRF-2006-005-J02102).

References

[1] V.I. Kudinov, I.L. Chaplygin, A.I. Kirilyuk, N.M. Kreines, R. Laiho, E. Lähderanta, C. Ayache, Phys. Rev. B 47 (1993) 9017.
[2] J.F. Federici, D. Chew, B. Welker, W. Savin, J. Gutierrez-Solana, T. Fink, W. Wilber, Phys. Rev. B 52 (1995) 15592.
[3] M. Osada, M. Käll, J. Bäckström, M. Kakihana, N.H. Andersen, L. Börjesson, Phys. Rev. B 71 (2005) 214503.
[4] M. Osada, M. Kakihana, M. Käll, J. Bäckström, L. Börjesson, N.-H. Anderson, Physica C 364–365 (2001) 545.
[5] E. Osquiguil, M. Maenhoudt, B. Wuyts, Y. Bruynseraede, D. Lederman, Ivan K. Schuller, Phys. Rev. B 49 (1994) R3675.
[6] A.G. Panfilov, A.I. Rykov, S. Tajima, A. Yamanaka, Phys. Rev. B 58 (1998) 12459.
[7] D.R. Wake, F. Slakey, M.V. Klein, J.P. Rice, D.M. Ginsberg, Phys. Rev. Lett. 67 (1991) 3728.
[8] C. Thomsen, M. Cardona, B. Gegenheimer, R. Liu, A. Simon, Phys. Rev. B37 (1988) R9860.
[9] V.G. Ivanov, M.N. Iliev, C. Thomsen, Phys. Rev. B 52 (1995) 13652.
[10] A. Fainstein, B. Maiorov, J. Guimpel, G. Nieva, E. Osquiguil, Phys. Rev. B 61 (2000) 4298.
[11] A. Fainstein, P. Etchegoin, J. Guimpel, Phys. Rev. B 58 (1998) 9433.
[12] M. Käll, M. Osada, M. Kakihana, L. Börjesson, T. Frello, J. Madsen, N.H. Andersen, R. Liang, P. Dosanjh, W.N. Hardy, Phys. Rev. B 57 (1998) R14072.
[13] Yijie Li, S. Linzen, F. Machalett, F. Schmidl, P. Seidel, Physica C 243 (1995) 294.

[14] B.W. Veal, A.P. Paulikas, H. You, H. Shi, Y. Fang, J.W. Downey, Phys. Rev. B 42 (1990) 6305.
[15] E. Osquiguil, M. Maenhoudt, B. Wuyts, Y. Bruynseraede, Appl. Phys. Lett. 60 (1992) 1627.
[16] J.A. Martínez, B. Wilkens, N.G. Stoffel, D. Hart, L. Nazar, T. Verkatesan, A. Inam, X.D. Wu, Appl. Phys. Lett. 57 (1990) 189.
[17] J.D. Jorgensen, M.A. Beno, D.G. Hinks, L. Soderholm, K.J. Volin, R.L. Hitterman, J.D. Grace, I.K. Schuller, C.U. Segre, K. Zhang, M.S. Kleefisch, Phys. Rev. B 36 (1987) 3608.
[18] P.V. Huong, J.C. Bruyere, E. Bustarret, P. Grandchamp, Solid State Commun. 72 (1989) 191.
[19] R. Feile, Physica C 159 (1989) 1.
[20] S. Degoy, J. Jiménez, P. Martin, O. Martinez, A.C. Prieto, D. Chambonnet, C. Audry, C. Belouet, J. Perrière, Physica C 256 (1996) 291.
[21] K. Conder, Mater. Sci. Eng. R 32 (2001) 41.
[22] R.M. Macfarlane, H.J. Rosen, E.M. Engler, R.D. Jacowitz, V.Y. Lee, Phys. Rev. B 38 (1988) 284.
[23] N. Poulakis, D. Palles, E. Liarokapis, K. Conder, E. Kaldis, K.A. Müller, Phys. Rev. B 53 (1996) R534.
[24] F.E. Bates, J.E. Eldridge, Solid State Commun. 64 (1987) 1435.
[25] C. Thomsen, M. Cardona, W. Kress, R. Liu, L. Genzel, M. Bauer, E. Schönherr, U. Schröder, Solid State Commun. 65 (1988) 1139.
[26] R. Liu, C. Thomsen, W. Kress, M. Cardona, B. Gegenheimer, F.W. de Wette, A.D. Kulkarni, Phys. Rev. B 37 (1988) 7971.
[27] A. Bock, R. Kürsten, M. Brühl, N. Dieckmann, U. Merkt, Phys. Rev. B 54 (1996) 4300.
[28] C. Greaves, P.R. Slater, Solid State Commun. 74 (1990) 591.
[29] A. Sacuto, M. Balkansk, J. Alloy. Compd. 195 (1993) 359.